We are IntechOpen, the world's leading publisher of Open Access books Built by scientists, for scientists

4,800
Open access books available

122,000
International authors and editors

135M
Downloads

Our authors are among the

154
Countries delivered to

TOP 1%
most cited scientists

12.2%
Contributors from top 500 universities

CLARIVATE ANALYTICS BOOK CITATION INDEX INDEXED

WEB OF SCIENCE™

Selection of our books indexed in the Book Citation Index in Web of Science™ Core Collection (BKCI)

Interested in publishing with us?
Contact book.department@intechopen.com

Numbers displayed above are based on latest data collected.
For more information visit www.intechopen.com

Chapter 5

An Integrated Land-Use System Model for the Jordan River Region

Jennifer Koch, Florian Wimmer, Rüdiger Schaldach and Janina Onigkeit

Additional information is available at the end of the chapter

http://dx.doi.org/10.5772/51247

1. Introduction

The Jordan River region (Israel, Jordan, and the Palestinian National Authority (PA)) is one of the most water scarce regions of the world. The total renewable water resource values in the Jordan River region are 52 to 535 m^3 per capita and year [15], which is far below the threshold value of 1000 m^3 per capita and year indicating chronic water scarcity [14]. On average, water resources withdrawn for agricultural activities, such as irrigated crop production, amount to two thirds of the total actual renewable water resources in the Jordan River region [17]. This makes the agricultural sector the region's major water user and shows the strong regional impact of agricultural land-use activities on water resources. Besides the effect on water resources, land-use activities also have a considerable effect on other natural resources [20]. Examples are desertification caused by maladjusted land management policies [1, 4], biodiversity loss due to habitat destruction and fragmentation [41, 64], and salinization of land induced by irrigation [22]. Current pressures on natural resources in the Jordan River region are likely to aggravate in the future due to high projected population growth rates, economic development, and changing climate conditions. This may cause a further degradation of the region's ecosystems and reduce their capacity to provide ecosystem services in the long run. Hence, there is an urgent need for a better understanding of the complex relationships in these human-environmental systems, in order to develop sustainable management strategies for the use of natural resources in the Jordan River region.

Water resources in the Jordan River region are largely transboundary and their distribution between Israel, Jordan, and PA is a potential source of conflicts. Hence, strategies for sustainable natural resource management in this region have to capture regulations at the state level and have to be based on consistent assessment methods and collaboration between the parties involved. This makes modeling approaches operating at the small scale or approaches focusing solely on natural systems unsuitable. However, existing integrated modeling approaches that cover the entire Jordan River region, such as presented in the Global Environmental Outlook 4 [58], apply spatial resolutions that are too coarse to capture the biophysical heterogeneity in the region, which is governed by a steep precipitation gradient [13].

In order to gain a better scientific understanding of the linkages between natural resources, land management, and ecosystem functioning in the Jordan River region, we developed the integrated modeling system LandSHIFT.JR (Land Simulation to Harmonize and Integrate Freshwater Availability and the Terrestrial Environment - Jordan River). LandSHIFT.JR is based on the spatially explicit land-use model LandSHIFT [49] and covers Israel, Jordan, and PA. It applies a cellular automata approach to calculate land-use changes and corresponding irrigation water requirements under current and future climate conditions. LandSHIFT.JR operates on a regular grid with a spatial resolution of 30 arc seconds. It was tailored specifically to the environmental and socio-economic conditions in the Jordan River region [28, 29]. Since scarce water resources, vegetation degradation due to overgrazing, detrimental effects of climate change on crop yields and irrigation water requirements, and increased soil salinity caused by irrigation are the major environmental issues in the Jordan River region, LandSHIFT.JR explicitly addresses these issues. This distinguishes LandSHIFT.JR from other integrated land-use modeling systems operating at a similar spatial resolution and scale, e.g. the CLUE(-S) model [61, 62]. LandSHIFT.JR simulates the spatial and temporal dynamics of land-use systems in the Jordan River region and allows exploring the impact of alterations in socio-economic and biophysical conditions on the spatial distribution and intensity of land-use activities and the feedback of land-use changes on socio-economic conditions. The modeling system's main field of application is the simulation of spatially explicit, mid- to long-term scenarios of land-use change. These scenarios show trends in land use and support the identification of hot spots of change and competition for land. Thus, spatially explicit land-use change scenarios generated with LandSHIFT.JR provide scientific support for evaluation and formulation of sustainable land-use planning and promote informed decision making.

The objective of this chapter is to provide a comprehensive description of the integrated modeling system LandSHIFT.JR and of its validation. Moreover, we present an example of an application of LandSHIFT.JR - a scenario-based assessment of land-use changes in the Jordan River region. In section 2, a short description of the biophysical conditions and the most important land characteristics of the Jordan River region is provided. In sections 3 to 5, a detailed description of LandSHIFT.JR is given. The description focuses on the underlying concepts of the modeling system as well as on the distinctive features of LandSHIFT.JR. The structure of these sections follows the "Overview, Design concepts, Details" protocol for model descriptions as proposed by [23] and is based on a description of an earlier version of LandSHIFT.JR [30]. Sections 6 and 7 provide overviews of the validation of LandSHIFT.JR and the results of an application example, respectively. The chapter closes with a discussion of and conclusions on the integrated modeling system, its validation, and simulation results in section 8.

2. The Jordan River region

LandSHIFT.JR was developed for Israel, Jordan, and PA (Fig. 1). The Jordan River region is bordered by Lebanon and Syria in the North, by Iraq and Saudi Arabia in the East, by Egypt in the Southwest, and by the Mediterranean Sea in the West. The region ranges from 34.22°E, 29.19°N to 39.30°E, 33.38°N. The terrain in the Jordan River region is very heterogeneous. The Coastal Plain, stretching along the Mediterranean Sea, is flanked by the Negev desert in the

Southeast and a mountainous region in the East and Northeast. In the North, the mountains force the coastal air masses to rise and, as a result, induce relatively high precipitation amounts [13]. A key physiographic feature of the Jordan River region is the Great Rift Valley in which the Jordan River, Lake Tiberias, and the Dead Sea are located. With 407 m below sea level, the Dead Sea marks the lowest point in the region and on the Earth's surface. The highland area in the Western part of Jordan, located along the Great Rift Valley, rises to elevations of 1200 m above sea level and drops gradually in elevation towards the East, where it develops into the Jordan desert plateau [13]. The point with the highest elevation in the Jordan River region is the Jabal Umm ad Dami, located in the South Jordan desert, with about 1854 m above sea level.

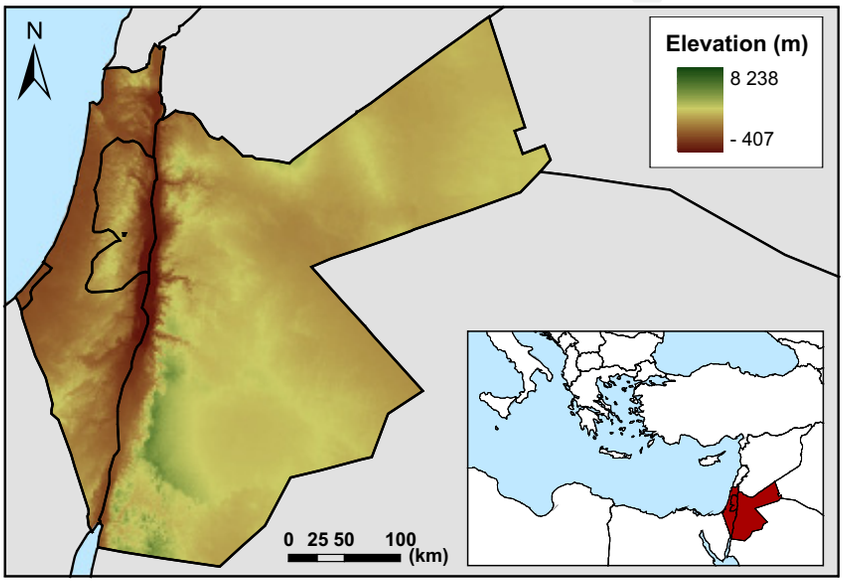

Figure 1. The study region covers Israel, Jordan, and the Palestinian National Authority.

The climate in the Northern, Central, and Western part of the Jordan River region is Mediterranean, characterized by hot, dry summers and cool winters [13]. In the residual part of the Jordan River region a semi-arid to arid climate predominates. A dominant feature of the regional climatic conditions is the steep precipitation gradient, ranging from 900 mm mean annual precipitation in the Northern tip of Israel to less than 50 mm in the desert areas in the South of Israel and the South and Southeast of Jordan. Temperatures also exhibit a high spatial variability across the Jordan River region with cold winters and hot summers in the mountainous regions and more moderate extremes in the Rift Valley and the Coastal Plain [13].

The Jordan River region covers about 116 thousand km^2 of land area and 1 thousand km^2 of inland water area. Approximately 76.1% of the land area in the region is located in Jordan, 18.7% in Israel, and 5.2% in PA [18]. About 2600 km^2 in the region are forest area. Arable land and permanent cropland sum up to about 9200 km^2. Approximately 3000 km^2 in the Jordan River region are equipped for irrigation. Thereof about two thirds are located in Israel. About 14 million people live in the Jordan River region [18]. The largest cities in the study region are Amman, Jerusalem, Tel Aviv, and Gaza.

3. Overview

3.1. Purpose

LandSHIFT.JR is a regional version of the integrated modeling system LandSHIFT [49]. It was adjusted and further developed to specifically simulate the spatial and temporal dynamics of land-use systems in the Jordan River region. LandSHIFT.JR was designed for exploring the effects of changes in socio-economic, climatic, and biophysical conditions on the spatial distribution and intensity of land-use activities. In addition, LandSHIFT.JR serves as a tool to formalize knowledge on and gain new insights into the functioning of land-use systems in the Jordan River region. It can be used to test hypotheses about processes and interlinkages within land-use systems, promote the understanding of these systems by identifying key processes and their interlinkages, and, as a result, reveal demands for future research activities.

LandSHIFT.JR's main field of application is the simulation of spatially explicit, mid- to long-term future scenarios of land-use and land-cover change. These scenarios explore possible trends in land use and visualize alternative land-use configurations. Main model output are maps displaying changes in land-use patterns. These maps help to reveal hot spots of land-use change and allow for the identification of priority areas for further research or focus areas for alternative management strategies. By these means, spatially explicit land-use change scenarios generated with LandSHIFT.JR provide scientific support for the evaluation and formulation of sustainable land-use planning and promote informed decision making.

3.2. State variables and scales

The representation of land-use systems in LandSHIFT.JR is operationalized on interacting spatial scale levels. On these scale levels, the state variables of the modeled land-use systems are defined. In total, there are four different spatial scale levels:

- **Macro level:** The spatial definition of the macro level is based on states. The state of a macro-level entity (i.e. a state) is specified by the state variables *population*, *crop demand*, *livestock number* (goats and sheep), *yield change* driven by technological progress, and *fraction of irrigated crop production* in total crop production. The state variables *crop demand*, *yield change*, and *fraction of irrigation area* are specified separately for each crop category. Changes in macro-level state variables constitute driving forces of land-use change in LandSHIFT.JR.
- **Intermediate level I:** The spatial scale hierarchy of LandSHIFT.JR includes a level based on natural regions. This scale level allows including information on crop demands with a higher spatial resolution such as the output from economic land-use models [26]. The only state variable specified on this level is *crop demand*. This state variable is specified separately for each crop category; a change in *crop demand* constitutes a driving force of land-use change in LandSHIFT.JR. *Crop demand* can only be specified on one spatial scale level. In case it is specified on the macro level, it cannot be specified on the intermediate level I and vice versa.
- **Intermediate level II:** The spatial configuration of the intermediate level II is specified by a regular grid with a spatial resolution of 0.02 decimal degrees (dd), which equals

approximately 2.2 km at the equator. The state variables defined on this level include potential *irrigated wheat yields*, potential *rainfed wheat yields*, and *net irrigation water requirements*. Changes in potential yields are considered to be drivers of land-use change.

- **Micro level:** The geographic area of each state is specified by the micro level - a regular grid with a uniform cell size of 30 arc seconds, which equals about 0.00833 dd or 1 km at the equator. The state of a micro-level grid cell is specified by the state variables dominant *land-use type*, *settlement area*, *population density*, *stocking density* for sheep and goats, *net primary productivity* (NPP) of rangeland and natural vegetation, *relative human appropriation of net primary production* (rel. HANPP [25, 29]), and *crop production*. The latter is defined separately for each crop category. Furthermore, a set of quasi-static landscape characteristics (e.g. slope) and land-use constraints (e.g. conservation areas) are defined on the micro level.

LandSHIFT.JR applies a 5-year time step. The length of the simulation period depends on the research question the respective simulation experiment is supposed to answer and typically ranges between 20 and 50 years. After each simulation step, LandSHIFT.JR writes the simulation results to files. This output comprises micro-level maps displaying the dominant land-use and land-cover type, population density, net irrigation water requirements, stocking density, and rel. HANPP. Moreover, the output includes a set of indicators and area statistics aggregated to the macro level.

3.3. Process overview and scheduling

The processes implemented in LandSHIFT.JR are organized in three modules (Fig. 2), which operate on the different spatial scale levels by modifying the scale-specific state variables. The **Biophysics module**, which describes the environmental subsystem, comprises process representations for the calculation of potential irrigated and rainfed wheat yields, net irrigation water requirements, and NPP of rangeland and natural vegetation. All the variables provided by the Biophysics module are climate dependent and, hence, differ between climate scenarios. This module operates on the intermediate level II and on the micro level. The **Socio-economy module** and the **Land Use Change module** (LUC module) represent the human subsystem. The Socio-economy module provides information on population growth, agricultural production and trade (implemented via the state variables crop demand and livestock numbers), and yield change due to technological progress. The processes of this module operate on the macro level and, in case crop demands are specified with a higher spatial resolution, also on the intermediate level I. For each simulation step, the Biophysics module and the Socio-economy module are executed and the corresponding state variables are updated. Subsequently, the updated information is used by the LUC module to simulate changes in land use and land cover. The processes of the LUC module operate on the micro level. Bidirectional information exchange between the modules is implemented via the exchange of the state variables.

The LUC module calculates the extent and location of land-use and land-cover changes. Therefore, it implements four land-use activities: housing and infrastructure, irrigated crop production, rainfed crop production, and livestock grazing. The processes representing the different land-use activities are organized in submodules: **METRO** for housing and

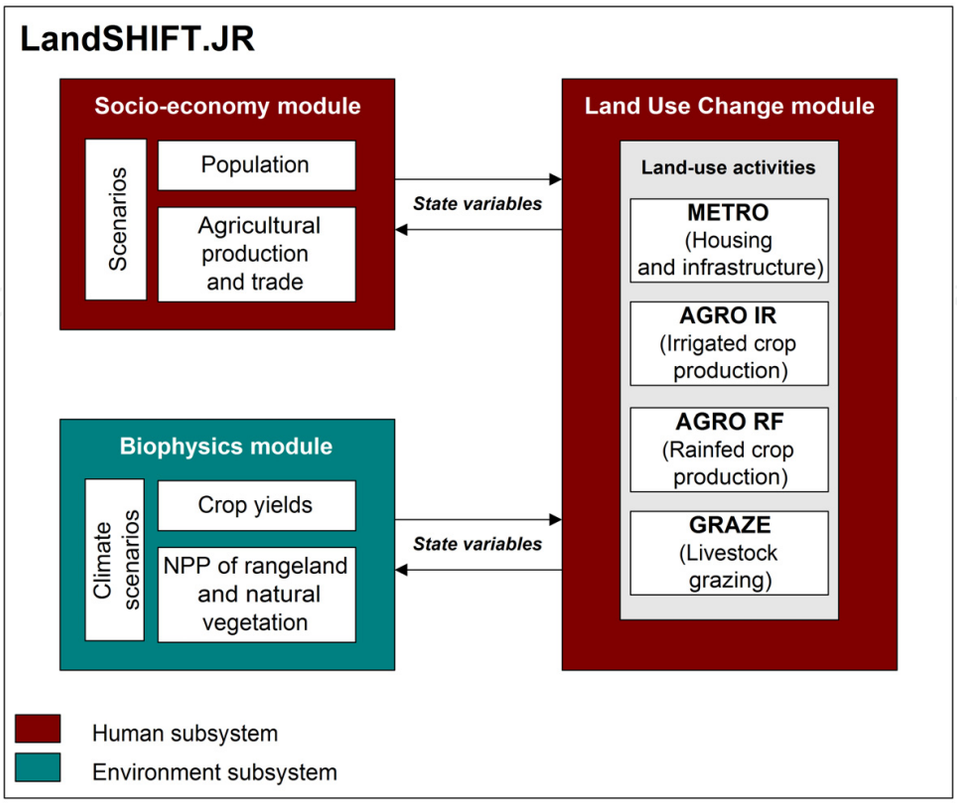

Figure 2. Conceptual structure of the integrated modeling system LandSHIFT.JR, adapted from [48].

infrastructure, **AGRO IR** for irrigated crop production, **AGRO RF** for rainfed crop production, and **GRAZE** for livestock grazing. The competition between these activities for land is addressed by a ranking of the four activities, which defines the sequence of execution. The ranking can be defined flexibly based on the research question; a straightforward way of ranking land-use activities is to follow their economic importance: METRO ▷ AGRO IR ▷ AGRO RF ▷ GRAZE. In one simulation step, cells occupied by a superordinate land-use activity are unavailable for a subordinate land-use activity.

In every simulation step, each land-use activity submodule executes the functional parts **demand processing**, **preference ranking**, and **demand allocation**. This complies with the generalized structure of spatially explicit land-use change models as presented by [63]. First, within the demand processing part, driving forces of land-use change are converted to macro-level/intermediate level I demands for services (e.g. housing) and agricultural commodities. Second, within the preference ranking part, the suitability of the micro-level grid cells for the different land-use activities is assessed, resulting in suitability maps. The grid cells are then ranked based on their suitability. Third, within the demand allocation part, each land-use activity manipulates the dominant land-use type as well as the corresponding state variable (population density for METRO, irrigated crop production for AGRO IR, rainfed crop production for AGRO RF, stocking density for GRAZE) of the best-suited micro-level grid cells, in order to meet the demand for the service or agricultural commodity under consideration. The range and magnitude of change is constrained by the demand for the service or agricultural commodity on the one hand and by the supply, i.e., the productivity on the particular micro-level grid cells on the other hand.

4. Design concepts

The choice of design concepts was guided by the purpose of the modeling system as described in section 3.1. LandSHIFT.JR combines a set of different design concepts that can be specified as a dynamic, integrated, process based, and spatially explicit.

Research questions that land-use modeling typically addresses are related to the timing and rate of land-use changes [35]. A prerequisite for the representation of the temporal behavior of land-use systems is a dynamic modeling approach [63]. LandSHIFT.JR applies such a dynamic modeling approach. It subdivides the simulation period into several time steps and, hence, fulfills the basic requirements for the simulation of land-use change trajectories, feedbacks, and path dependencies in the evolution of land-use systems.

According to [2], integrated modeling systems have to include information from more than one discipline, organize information in a modularized program structure, and link scientific findings with policy analysis. LandSHIFT.JR was developed to bring together information from different disciplines to support decision making and it is typically applied in the context of scenario analyses with strong relevance for land-use planning and policy [29, 31]. Furthermore, it provides a framework for the combination of biophysical and socio-economic information with geographic information in form of a modularized program structure.

LandSHIFT.JR applies a process-based modeling approach in order to describe the land-use systems of the Jordan River region as human-environmental systems and to explore the interlinkages between their subsystems. The modeling system includes representations of the key processes resulting in changes in human-environment systems. As pivotal process, LandSHIFT.JR implements human decision making with regard to the extent, location, and intensity of land-use activities. The process-based approach allows analyzing trajectories and intermediate states of land-use and land-cover change [63].

Spatially explicit land-use models simulate changes in land use for individual spatial entities [63]. In case of LandSHIFT.JR these spatial entities are cells of a regular grid. Spatially explicit models, such as LandSHIFT.JR, are able to simulate the location and spatial variability of land-use and land-cover changes and, as a result, enable the analysis of the interlinkages between socio-economic and biophysical environments as well as variations in location and quantity of land use.

5. Details

5.1. Initialization

Since LandSHIFT.JR integrates data from different fields and sources, considerable effort is required to synchronize the different datasets in an initial simulation step. In order to harmonize the information on population density and the land-use/land-cover map information on urban areas, LandSHIFT.JR initially reads the basic land-use/land-cover map (derived from the MODIS global land cover dataset [21]). This information is then combined with the micro-level information on population density [8]. On micro-level grid cells, at which the land-use type is not “urban”, but where the population density exceeds the upper limit for population density in rural regions, the land-use type is changed to “urban”. Furthermore,

spatial information on population density is combined with information on per capita area demands [12] in order to calculate the settlement area on non-urban grid cells; this area is not available for land-use activities such as crop production or livestock grazing.

Available land-use/land-cover map products for the Jordan River region do not distinguish between area under crop for different crops. Furthermore, grazing areas are not assigned separately. Hence, an initial distribution of rangeland as well as area under crop for the considered crop categories has to be generated artificially. In order to derive the initial distribution of area under crop, LandSHIFT.JR distributes areas for the different crop categories to the best suited micro-level grid cells (see section 5.3.3). These areas under crop are derived from national statistics for Israel[1], Jordan[2], and PA[3] for the year 2000. Based on the MIRCA2000 dataset [44], double cropping is assumed for rainfed and irrigated vegetables in all three states. The applied area values are displayed in Table 1. The best suited micro-level grid cells, on which these areas are distributed, are preferably those cells that are categorized as "cropland" in the underlying land-use/land-cover map. The distribution of areas under crop is carried out separately for irrigated and rainfed crop production. In case grid cells categorized as "cropland" in the underlying map are not categorized as one of the considered crop categories during initialization, their land-use type is set to "other crops" and kept static for the rest of the simulation run. This is based on the assumption that "cropland" in the original land-use/land-cover map also includes areas covered with crops that are not contained in one of the considered categories and that for these crops no drivers are specified as model input.

State	IR fruits	IR vegetables	IR cereals	RF fruits	RF vegetables	RF cereals	Rangeland
	[km^2]	[km^2]	[km^2]	[km^2]	[km^2]	[km^2]	[km^2]
Israel	661.4	253.6	643.0	162.6	22.1	1206.9	1480
Jordan	348.2	155.3	110.3	521.3	9.1	1045.5	7910
PA	81.6	67.1	26.8	1092.9	19.9	440.4	1500

Table 1. Cropland and rangeland areas derived from national statistics and FAOSTAT [18] used to initialize cropland and rangeland area distribution in LandSHIFT.JR.

Based on the resulting land-use type distribution, LandSHIFT.JR relates the macro-level production $pcens_c$ for each of the irrigated and rainfed crop categories c (derived from census data) to the sum of the local production on grid cells with that crop category in the newly generated map $pcalc_c$. This is done in order to calculate a separate management parameter $base_c$ for each of these categories. The management parameter is defined as $base_c = pcens_c / pcalc_c$. It accounts for inconsistencies between different data sources and uncertainties due to agricultural management strategies (e.g. multiple cropping, fertilization) that affect the total production of a crop but are not explicitly considered in LandSHIFT.JR. Crop production values applied in this context are[4]: about 1.78 million tonnes of fruits (Israel: 1.304 million tonnes, Jordan: 0.232 million tonnes, PA: 0.246 million tonnes), about 3.01 million tonnes of vegetables and melons (Israel: 1.643 million tonnes, Jordan: 0.825 million tonnes, PA: 0.541 million tonnes), and about 0.27 million tonnes of cereals (Israel: 0.183 million

[1] http://www1.cbs.gov.il/reader/cw_usr_view_Folder?ID=141
[2] http://www.dos.gov.jo/dos_home_e/main/index.htm
[3] http://www.pcbs.gov.ps/Default.aspx?tabID=1&lang=en
[4] All values derived from FAOSTAT are given as 3-year average for the years 1999-2001.

tonnes, Jordan: 0.044 million tonnes, PA: 0.041 million tonnes). The crop specific management parameter is evaluated for initial conditions and is applied in the following simulation steps in order to adjust the yield values and, as a result, transfer potential crop yields into actual yields. Based on irrigated area under crop, rainfed area under crop, and the adjusted crop yields, the fraction of irrigated crop production in total crop production is calculated. This parameter is also invariant.

There are two different modes available in LandSHIFT.JR for calculating the initial distribution of rangeland and the related stocking densities for small ruminants: a production-driven approach and an area-driven approach. For the production-driven approach, the forage demand is allocated to the best suited micro-level grid cells and the land-use type of these cells is converted to "rangeland". The forage demand is calculated from livestock numbers derived from statistical data and the forage demand per animal [40]. Livestock numbers used in this context were derived from FAOSTAT [18] and amount to 0.4 million sheep and goats in Israel, 2.2 million sheep and goats in Jordan, and 0.9 million sheep and goats in PA. For the area-driven approach, rangeland area for the year 2000 (also derived from FAOSTAT, Table 1) is allocated to the best suited micro-level grid cells. The land-use type of these grid cells is set to "rangeland". The stocking densities on the rangeland cells are then calculated from the local NPP of rangeland and natural vegetation and the forage demand per sheep or goat.

5.2. Input

LandSHIFT.JR input comprises time series on population, crop demands, yield change due to technological progress, livestock numbers as well as socio-economic information, e.g. on environmental policies or regional planning. For the application example presented in this chapter, this information is derived from the participatory scenario exercise of the GLOWA Jordan River project[5]. An overview of the scenarios and the corresponding values for the drivers of land-use change is given in [6]. Besides the above mentioned input specified on the macro level and/or intermediate level I, LandSHIFT.JR requires data on landscape and land-use characteristics specified on intermediate level II and on the micro level. This category of input includes potential crop yields and NPP under current and future climate conditions or landscape attributes such as slope or river network density. A detailed description of the data input on landscape and land-use characteristics is given in section 5.3.4.

5.3. Submodels

The processes in LandSHIFT.JR are organized in the three submodels Biophysics module, Socio-economy module, and LUC module. The details of these submodels are described in this section.

5.3.1. Biophysics module

In each simulation step, the Biophysics module updates the state variables potential irrigated wheat yields, potential rainfed wheat yields, net irrigation water requirements, and NPP of rangeland and natural vegetation. The updated information is then provided to the LUC

[5] http://www.glowa-jordan-river.de

module. The calculation of wheat yields and irrigation water requirements is based on the output of the dynamic, process-based crop growth model EPIC [67, 68]. In order to include future progress in the agricultural sector such as new management methods or fertilizers into the crop yield calculations, yields are corrected with a state-specific factor for yield change due to technological progress. The calculation of the state variable NPP of rangeland and natural vegetation is based on output of WADISCAPE [34]. In contrast to the wheat yield calculations, no effect of technological change on productivity is taken into account. This is based on the assumption that small ruminant grazing in the Jordan River region usually takes place on largely unmanaged marginal lands. The impact of changing climate conditions is considered for wheat yields, irrigation water requirements, and NPP. This is realized by a correction for climate change based on a linear interpolation between the productivities or water requirements calculated for current climate conditions and the respective productivities or water requirements calculated for future climate conditions given by regional climate simulations for the Jordan River region [53].

GEPIC. We applied GIS-based EPIC (GEPIC) [37], a combination of the crop growth model EPIC [67, 68] with a GIS, to simulate wheat yields and crop water requirements under current and future climate. EPIC has been used successfully to simulate crop yields under a wide range of weather conditions, soil properties, and management schemes [37]. EPIC works on a daily time step and considers the major processes in the soil-crop-atmosphere-management system [67]. We used simulated potential yield under rainfed and optimal irrigated conditions for wheat as a proxy crop type. In order to derive irrigated/rainfed yields for the crop categories fruits, vegetables, and cereals from irrigated/rainfed wheat yield, an additional processing step was required. We multiplied the grid cell values of potential wheat yield by the ratio of mean actual yield for an irrigated/rainfed crop category to the mean potential yield on irrigated/rainfed areas covered by the crop category. This step was based on values for the year 2000. The actual yields stem from IMPACT model [45] calculations that were also used to provide input on future crop production. By this means, we ensure the consistency of yield values between the various model drivers and inputs. At the same time, we are able to include spatial and temporal variability of the crop yield simulations with GEPIC in our analysis.

WADISCAPE. The WADISCAPE model [34] provides information on stocking capacities[6] as well as information on the relationship between stocking density with small ruminants (goats and sheep) and productivity of green biomass[7] under current and future climate conditions. WADISCAPE simulates the growth and dispersal of herbaceous plants and dwarf shrubs in artificial, fractal wadi landscapes (wadiscapes) of 1.5 km $\times$ 1.5 km. The main exogenous driver of vegetation dynamics in WADISCAPE is water availability, which is calculated from precipitation under consideration of topography. The simulation of vegetation dynamics is based on validated small-scale models of annual plants [33, 34] and dwarf shrubs [38]. WADISCAPE simulations were conducted for five climatic regions (arid to mesic Mediterranean) and, in factorial combination, five varying slope categories (0° to

[6] Stocking capacity is defined as the number of sheep and goats per hectare for which the green biomass production provides enough food in nine of ten years in year-round grazing [34].

[7] In this context, green biomass is defined as the aboveground biomass of herbaceous plants and leaf mass of dwarf shrubs.

30°). In order to determine the stocking capacity of the vegetation, these simulations were conducted for stocking densities ranging from 0 to 10 animals per hectare.

5.3.2. Socio-economy module

The Socio-economy module operates on the macro level and, if crop demand information with a higher spatial resolution is included, additionally on the intermediate level I. The module accounts for the organization and processing of the state variables population, crop demand, livestock number, and changes in crop yield due to technological progress. For historical periods, information on these state variables is derived from statistical databases (e.g. FAOSTAT [18]). For future periods, this information is typically generated with participatory scenario development, following the SAS approach [3] and the economic model IMPACT [45]. An update of the state variables is carried out by the Socio-economy module within each simulation step.

IMPACT. The International Model for Policy Analysis of Agricultural Commodities and Trade (IMPACT), a representation of a competitive global market for agricultural commodities [45], was designed for the analysis of current conditions and possible future developments in food demand, supply, trade, prices, and malnutrition outcomes. The model covers 32 commodities and 36 countries/regions linked through trade and, hence, accounts for almost all of the world's food production and consumption. IMPACT is based on a system of supply and demand elasticities implemented via linear and nonlinear equations. It incorporates demand as a function of price, income and population growth, and changes in crop production. The changes in crop production are determined on the basis of crop prices and productivity growth rates [45].

SAS. The SAS (Story And Simulation) approach to scenario analysis [3] combines both, quantitative and qualitative aspects of scenarios. The combination of those two aspects makes the resulting scenarios on the one hand generally understandable and on the other hand suitable for planning purposes. Distinctive features of SAS are the iterative structure and the intensive participation of experts and stakeholders. A detailed description of SAS is provided by [3]; a description of the SAS application in the context of a scenario analysis for the Jordan River region is given in [6]. Results from this scenario analysis were used to derive information on future development of population and livestock numbers in the Jordan River region for the application example (see section 7).

5.3.3. Land Use Change module

The LUC module is the central component of LandSHIFT.JR. The module accomplishes the simulation of the location and quantity of land-use and land-cover changes. This is realized by a regionalization of the macro-level/intermediate level I demands for area intensive services and agricultural commodities to the micro level. The basic principle is to allocate the demands to the most suitable micro-level grid cells by changing the land-use type, population density, crop production or livestock density of as many cells as required to meet the demand. Each service or commodity is linked to a land-use type. The LUC module implements the submodules METRO (housing and infrastructure), AGRO IR (irrigated crop production), AGRO RF (rainfed crop production), and GRAZE (livestock grazing). In every simulation

step, these four submodules are executed subsequently and each of this submodules executes the three functional parts demand processing, preference ranking, and demand allocation. In the following, the general operating mode of the functional parts is described.

Demand processing. The functional part demand processing is responsible for the transformation of the drivers of land-use change to macro-level/intermediate level I demands for the implemented services and commodities.

Preference ranking. The functional part preference ranking operates on the micro level and serves for the identification and ranking of the preferred grid cells for the different land-use activities and the corresponding land-use types. A method from the field of Multi Criteria Analysis [11] is applied in order to calculate the preference values of the grid cells for the different land-use types. The preference value ψ_k of a grid cell k is calculated as

$$\psi_k = \underbrace{\sum_{i=1}^{n} w_i f_i(p_{i,k})}_{\text{suitability}} \times \underbrace{\prod_{j=1}^{m} g_j(c_{j,k})}_{\text{constraints}} \tag{1}$$

with $\sum_i(w_i) = 1$ and $f_i(p_{i,k})$, $g_j(c_{j,k}) \in [0,1]$. The first part of the equation is the sum of the different weighted suitability factors p, contributing to the suitability of a grid cell k for a particular land-use type. The weights w determine the importance of a suitability factor in the analysis. The factor weights were determined according to the CRITIC method [10]. This method allows the calculation of "objective weights" on the basis of the contrast intensity between the evaluation criteria, i.e., the standard deviation of normalized criteria values and the inter-criteria correlation. The second term of the equation is the product of the land-use constraints c. These constraints reflect important aspects of human decision making, e.g. land-use restrictions in conservation areas. One constraint implemented in LandSHIFT.JR is the transition between the different land-use types: not all land-use and land-cover types can be converted into each other. These conversion elasticities are a frequently used method in the field of land-use modeling [62]. A summary of all possible conversions is given in Table 2.

From / To	Urban	IR cropland	RF cropland	Rangeland	Set aside	Natural veg.
Urban	+	-	-	-	-	-
IR cropland	+	+	-	-	+	-
RF cropland	+	+	+	-	+	-
Rangeland	+	+	+	+	-	-
Set aside	+	+	+	+	+	-
Natural veg.	+	+	+	+	-	+

Table 2. Land-use transition matrix. Possible conversions are indicated by "+", impossible conversions are indicated by "-".

The suitability factors, their weights, and the land-use constraints are specified on the macro level and implemented as time-dependent variables. This enables the representation of changing policies and environmental boundary conditions. Suitability factors and constraints are normalized by factor-specific value functions f and constraint specific value functions g. Value functions, based on logistic regression analysis, can be defined as positive or negative

relationships and are scaled by the range of the respective factor within a state in order to account for the spatial heterogeneity.

Suitability factors and constraints can be state variables, landscape attributes, zoning regulations, or spatial neighborhood characteristics. The neighborhood of the micro-level grid cells is analyzed in each simulation step in order to generate information about the land-use/land-cover type of the adjacent cells. The neighborhood of a cell can be defined by type and order, e.g. von Neumann or Moore neighborhood. Additionally, a (geographic) search radius can be specified. The set of relevant suitability factors and land-use constraints, the types of value functions, and the factor weights can be derived either by data driven procedures (e.g. geostatistical analysis) or by expert knowledge (e.g. by means of the Analytical Hierarchy Process [46]).

Demand allocation. The functional part demand allocation assigns the macro-level and intermediate-level I demands for the implemented services and commodities to the micro-level grid cells with the highest preference for the associated land-use type. For this functional part, each land-use activity implements its own allocation strategy:

- **METRO.** The submodule METRO simulates the spatial and temporal dynamics of area for housing and infrastructure. Changes in quantity and location of this area are driven by alterations in population numbers, specified on the macro-level. The demand allocation procedure for METRO distinguishes between municipal regions and rural regions. Depending on the category, a different kind of growth process is applied. Therefore, the micro-level grid cells are grouped into these two categories. A municipal cell is defined as a cell that features the land-use type "urban" or has at least one grid cell with the land-use type "urban" in its direct neighborhood. All other cells are defined as rural cells. The growth of urban areas is implemented as urban encroachment process [69], i.e., new area for housing and infrastructure is located at the edges of existing urban area [54].

  In order to allocate additional population, a three-step procedure is applied. First, a parameter defines the fractions of the additional population that is assigned to municipal and rural regions, respectively. Second, depending on the grid cell's actual population density and suitability values, additional population is allocated. On cells with the land-use type "urban", an upper threshold for population density is defined, which limits the population amount that can be allocated to these grid cells. Third, based on the recalculated population densities, land-use conversions are calculated: rural cells feature a threshold value for population density. In case, this population density value is exceeded, the land-use type of the grid cells is changed to "urban".

  In rural regions, each cell has a fraction of settlement area that is occupied by housing and infrastructure. The amount of settlement area on a rural grid cell is calculated based on population density and the per capita area demand [12]. The area not required for housing and infrastructure is available for other land use or land cover that specifies the dominant land-use type on rural grid cells. On grid cells with the dominant land-use type "urban", all area is required for housing and infrastructure.

- **AGRO IR and AGRO RF.** The two AGRO submodules AGRO IR and AGRO RF are separate submodules that are executed one after another (see section 3.3). AGRO IR is

responsible for the allocation of the crop categories irrigated fruits (excluding melons), irrigated vegetables and melons, and irrigated cereals. AGRO RF allocates the crop categories rainfed fruits (excluding melons), rainfed vegetables and melons, and rainfed cereals. The crop category definition is based on the crop type aggregation of the FAOSTAT database [18]. Both, AGRO IR and AGRO RF, follow the same general approach regarding demand allocation, and are hence described jointly.

The basic principle of the demand allocation part in AGRO is to formulate a "compromise-solution"-problem for the calculation of a quasi-optimum crop allocation, in order to deal with the competition for land resources between the different crop categories. This is implemented as a modified version of the Multi-Objective Land Allocation (MOLA) heuristic [11]. This heuristic resolves emerging conflicts by a pair-wise comparison; cells claimed by more than one crop category are allocated to the category with the higher preference value. In LandSHIFT, the heuristic was modified in two ways [49]. First, the modified version allocates crop demands instead of a given area. Second, pattern stability is considered in the conflict resolution step, i.e., the land-use patterns remain constant if no changes in crop demands occur.

The amount of crop production on a micro-level grid cell is based on the local production P. The local production P for a crop category c at simulation step t for a particular grid cell, is defined as:

$$P_c(t) = base_c \times y_c(t) \times (1 + tech_c(t)) \times a_c(t) \quad (2)$$

$P_c(t)$ micro-level grid cell production of crop category c for simulation step t [Mg],
$base_c$ management parameter for crop category category c [-],
$y_c(t)$ micro-level grid cell yield for crop category c in simulation step t [Mg km^{-2}],
$tech_c(t)$ technology-induced yield change for crop category c in simulation step t [-],
$a_c(t)$ available cell area for production of crop category c in simulation step t [km^2].

The crop production P is computed by combining state variables from different spatial scale levels (crop yield and yield change) and the cell area a that is not used as settlement area. The local crop yield is updated in each simulation step by the Biophysics module in order to include changes due to alterations in climatic conditions. The management factor *base* is a proxy for agricultural management characteristics (see section 5.1), which are not directly taken into account by LandSHIFT.JR. If not enough suitable land resources are available to allocate the crop demands, unmet demands are documented in a text file. In case more cropland was allocation in a previous simulation step as required in the following simulation step, the land-use type of dispensable cells is converted to "set aside" (fallow).

- **GRAZE.** The GRAZE submodule accounts for the spatial and temporal dynamics of livestock grazing. Changes in quantity and location of grazing area, which has the land-use type "rangeland", are driven by alterations in livestock numbers (sheep and goats) given in livestock units (LU), specified on the macro-level. Based on the livestock number, the amount of required forage, which has to be provided by grazing land, is calculated. This is done under consideration of the daily forage demand per LU and the share of grazing in feed composition. The residual share in feed composition is assumed to be covered by crops and crop residues and is considered indirectly in LandSHIFT.JR.

  The demand allocation part of GRAZE is based on a relationship between grazing intensity (stocking density) and local biomass productivity (NPP of rangeland and natural

vegetation). This relationship is specified by non-linear correlation functions between stocking density (number of small ruminants per hectare) and green biomass productivity (tonnes per hectare), calculated with WADISCAPE [34]. The correlation functions were generated for all combinations of five slope categories (0° to <5°, ≥5° to <12.5°, ≥12.5° to <17.5°, ≥17.5° to <25°, ≥25°) with five categories of mean annual precipitation (Table 3). Areas with mean annual precipitation values, that are not covered by the WADISCAPE simulations (values below 80 mm mean annual precipitation) are not suitable for livestock grazing. Except for micro-level grid cells located in these areas, each micro-level grid cell is attributed to one of the correlation functions depending on the grid-cell value for slope and mean annual precipitation.

Category	Mean annual precipitation [mm]
Arid	≥ 80 to < 200
Semiarid	≥ 200 to < 400
Dry Mediterranean	≥ 400 to < 500
Typical Mediterranean	≥ 500 to < 700
Mesic Mediterranean	≥ 700 to < 960

Table 3. Mean annual precipitation categories in WADISCAPE [34].

Two different allocation routines are available for calculating the initial distribution of rangeland and the corresponding stocking densities:

1. Demand-driven approach: The forage demand is allocated to the preferred micro-level grid cells and the land-use type of these cells is converted to "rangeland". The local biomass productivity is calculated from the non-linear correlation function that is valid for the respective grid cells, assuming no former grazing activity on these grid cells. Based on the available biomass productivity, the local stocking density is calculated under consideration of the forage demand per animal.
2. Area-driven approach: Instead of a forage demand, a certain amount of rangeland area (Table 1) is allocated to the micro-level grid cells. The land-use type of these grid cells is converted to "rangeland". The potential total biomass production on these grid cells is calculated from the non-linear correlation functions, assuming no former use of these cells as rangeland. Based on the potential biomass production on the resulting area, the stocking density is adjusted and assigned to the grid cells, in order to meet the forage demand.

In order to calculate the local biomass productivity in the following simulation steps, the cell's correlation function is chosen and combined with the stocking density set in the initial simulation step. The actual stocking density is then calculated from this productivity via the forage demand and assigned to the grid cell. In the subsequent simulation step, this stocking density is then used to derive the new local productivity from the cell specific correlation function. This procedure is repeated for each simulation step [29].

An important effect of this feedback between stocking density and biomass productivity is the resulting self-regulation of the grazing system: the allocation of high stocking densities in one simulation step results in reduced biomass productivity in the following simulation step and, hence, lower stocking densities. In addition to the dynamic calculation of local

biomass productivity, change in biomass productivity due to climate change, also derived from WADISCAPE calculations driven by regional climate simulations [53], is considered.

The GRAZE demand allocation part features two different methods for rangeland management: (1) sustainable rangeland management and (2) intensive rangeland management [29]. These allocation modes use micro-level grid cell specific information on stocking capacities calculated by WADISCAPE. The allocation modes apply different procedures in case the local stocking density exceeds the stocking capacity (overgrazing). In case of sustainable management, the local sustainable stocking capacity defines the maximum possible stocking density at a grid cell. The sustainable stocking capacity is a user defined fraction of the maximum stocking capacity. Each time the stocking density, assessed from local biomass productivity, exceeds the sustainable stocking capacity of the grid cell, the stocking density is set back to the sustainable stocking capacity, i.e., no overgrazing is allowed. For intensive management, this limitation is not applied and the stocking density is exclusively limited by the local biomass productivity. For both managements, the upper limit for stocking density is 10 animals per hectare, given by the range of the WADISCAPE simulations [34].

Besides the above mentioned land-use/land-cover types urban, irrigated fruits (excl. melons), irrigated vegetables (incl. melons), irrigated cereals, rainfed fruits (excl. melons), rainfed vegetables (incl. melons), rainfed cereals, other crops, set aside, and rangeland, a set of other types exist. These are: forests, cropland/natural vegetation mosaic, grassland, shrub land, woody savannah, barren land, water, and wetlands. Changes in those are not directly simulated by LandSHIFT.JR but result from land-use conversions of the land-use types that area covered by METRO, AGRO, and GRAZE.

5.3.4. Submodel parameterization

METRO. For METRO, two suitability factors were considered: terrain slope [59] and travel time to major cities [57]. In Table 4, all suitability factors and their weights for the different land-use activities are displayed. As land-use constraint, conservation areas were implemented. As a result, no new urban area can be allocated in conservation areas. Spatially explicit information on national and international nature conservation area was derived from the World Database on Protected Areas [66]. The basic principle of METRO is to convert the population to a cell specific population density value. For this purpose, one part of the population is allocated to urban areas; the residual part is allocated to rural areas. The fraction of population allocation to urban areas is 65 % [58]. In case that the rural population density exceeds 5000 people/km^2, or the area demand for housing and infrastructure on a grid cell exceeds 80 % of the grid cell size, the land-cover type of the grid cell is changed to "urban". The maximum population density per grid cell is 26098 people/km^2, derived from the population density map for the study region for the year 2000 [8].

AGRO IR. For AGRO IR, six different suitability factors were considered. Besides terrain slope and travel time to major cities, additionally area equipped for irrigation [52], irrigated crop yields, population density, and river network density were considered. Irrigated crop yields were calculated with GEPIC and vary with time based on changes in climate conditions. Population density for the year 2000 is derived from the CIESIN dataset [8] and is updated by

Activity	Suitability factor	Factor weight
METRO	Terrain slope	0.366
	Travel time to major cities	0.634
AGRO IR	Area equipped for irrigation	0.233
	Irrigated crop yield	0.145
	Population density	0.049
	River network density	0.262
	Terrain slope	0.147
	Travel time to major cities	0.164
AGRO RF	Population density	0.067
	Rainfed crop yield	0.311
	Terrain slope	0.258
	Travel time to major cities	0.364
GRAZE	Population density	0.044
	NPP of rangeland/nat. veg.	0.529
	River network density	0.256
	Terrain slope	0.170

Table 4. Suitability factors and corresponding weights for the different land-use activities.

LandSHIFT.JR over the course of the simulation. The river network density is calculated as the line density of rivers per grid cell, based on the RWDB2 river-surface water body network dataset [19]. As land-use constraints, conservation areas are considered. Furthermore, a risk map on soil sensitivity to adverse effects of irrigation with treated wastewater [47] was included and can be used for future studies.

AGRO RF. For AGRO RF, four suitability factors were considered. These are rainfed crop yields, slope, travel time to major cities, and population density. Rainfed crop yields were calculated with GEPIC and vary with time based on changes in climate conditions. The only land-use constraint for this activity is conservation area.

GRAZE. For GRAZE, the four considered suitability factors are NPP on rangeland and natural vegetation, slope, river network density, and population density. In conservation areas, the use as rangeland is constrained. The information on NPP is derived from WADISCAPE calculations. To derive the forage demand from the livestock number, we assume one sheep or goat to equal 0.125 LU [51]. In addition, we apply a regional factor for Israel (0.8) and Jordan/PA (0.42) that considers the geographical variability in animal body size [51]. The daily forage demand per goat or sheep is 1.35 kg dry matter [40] of which we assume 30 % to be covered by grazing [4]. The consumable part of the aboveground green biomass is 75 %.

6. Model validation

We applied three different methods to validate our modeling system. First, we validated the underlying assumptions of the suitability assessment with the Relative Operating Characteristics (ROC) method [43]. Second, we used the MODIS land cover dataset for the

years 2001 and 2005 to perform a map comparison analysis using version 2.0 of the Map Comparison Kit[8]. Third, we compared macro-level simulation results on area under crop for the different irrigated and rainfed crop categories for the year 2005 with the corresponding values from statistical databases.

6.1. Relative Operating Characteristics

The agreement of simulated and observed land-use change depends on the agreement of both the quantity and location of change. Only if the simulated quantity of change equals the observed quantity of change, the simulated land-use changes can agree perfectly with the real land-use changes. On contrary, if the simulated quantity of change equals the observed quantity of change the location of simulated change can still lead to disagreement of modeled and real land-use change.

The ROC method [43] allows assessing to what degree the model is capable to assess the right location of change independently of the simulated quantity of change. Hence, the ROC analysis can be used to validate the underlying preference ranking processes that guide the location of changes in land use and land cover, represented by a suitability map. For this purpose, an independent real-change map indicating observed land-use or land-cover changes is necessary. Since the ROC method is only meaningful for testing the suitability map for the conversion of any land-use/land-cover type to one single land-use/land-cover type at a time, we applied the method to validate the suitability maps for each land-use activity separately. Whereas the suitability map for a specific land-use activity is a direct model output of LandSHIFT.JR, the categorical real-change map had to be constructed. For this purpose, observed raster maps for two points in time were compared to each other. Grid cells that feature a land-use or land-cover change between these two points in time were categorized as *change* cells whereas all other cells are categorized as *non-change* cells.

The ROC method compares the real-change map to a sequence of virtual simulated land-use change maps that result from a successively increasing quantity of change. The maps are derived by assuming that land-use change occurs on cells where the suitability value exceeds a certain threshold. Typically, the minimum, the deciles, and the maximum of the distribution of the suitability values are used as thresholds to prepare a sequence of maps assuming land-use change on 0 % to 100 % of all cells in 10 %-steps. In order to compare each of these maps to the real-change map, the rates of true positives (TP) and false positives (FP) are calculated. A cell is counted as a TP if real land-use change is modeled correctly. In contrast, if simulated land-use change coincides with non-change in reality, the cell is counted as a FP. The rates of TP and FP are computed as the ratio of the number of TPs and the number of possible TPs and the ratio of the number of FPs and the number of possible FPs, respectively. Based on the results of each comparison in the sequence, the ROC-diagram is constructed by plotting a curve in a coordinate system with the FP-rate on the x-axis and the TP-rate on the y-axis. The ROC curve starts at the point (FP = 0, TP = 0), resulting from the assumption of zero simulated land-use change, and ends at the point (FP = 1, TP = 1), resulting from the assumption that land-use change is simulated on all cells. The performance metric of ROC, the area under the curve (AUC), is calculated by trapezoidal approximation. On average, a random suitability

[8] http://www.riks.nl/products/Map_Comparison_Kit

assessment results in a value of AUC = 0.5. In contrast, a suitability map that assigns the n highest values to the n cells where real change occurs (the perfect suitability map) yields AUC = 1. Hence, an AUC-value between 0.5 and 1 indicates that the suitability assessment explains the location of change better than a random process.

We performed three separate ROC analyses for the land-use activities METRO, AGRO, and GRAZE. Therefore, we compiled three different real-change maps. For METRO and AGRO, we used the MODIS land cover dataset for the years 2001 and 2005. All cells that were "urban" ("cropland") in the 2005 map but not in the 2001 map are categorized as change for METRO (AGRO). For GRAZE, the real change map was derived from the small ruminant density (SRD) maps adjusted to match FAO totals for the years 2000 and 2005 [16]. We defined real change from non-grazing to grazing if the small ruminant density increases by 25% and by a minimum of 25 animals per km^2 over the five year period. The ROC curves resulting from the analyses are shown in Fig. 3.

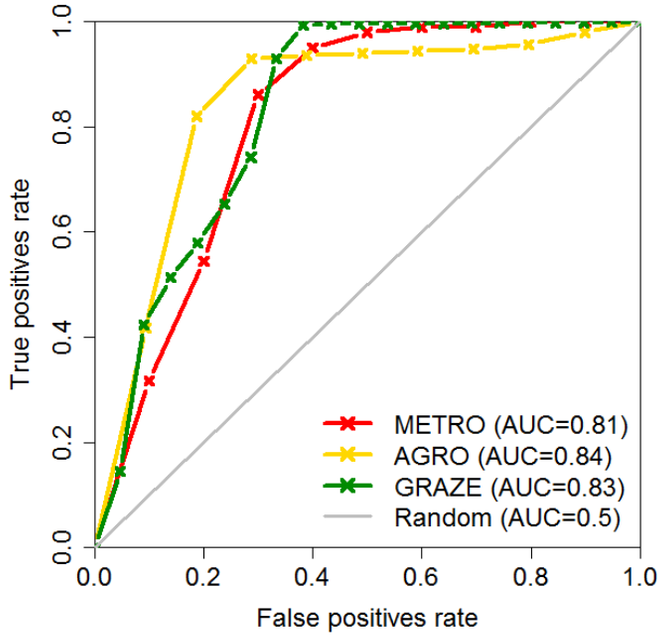

Figure 3. Relative Operating Characteristics (ROC) curves for the three land-use activities METRO, AGRO, and GRAZE. The 45° line indicates the ROC curve for randomly distributed suitability values. The area under the curve (AUC) is the performance measure of ROC.

6.2. Map comparison analysis

We carried out a map comparison analysis to validate the resulting land-use maps. For this purpose, we compared the simulated land-use map S for the year 2005 with the MODIS land cover map for the same year, which we considered the actual or reference land-use map A, by calculating the kappa coefficient of agreement (κ) [9, 42] and kappa simulation (κ_{sim})[60].

We applied κ because it is commonly used for validation of simulated land-use maps. The coefficient takes into account that the proportion of cells that are classified correctly by chance, denoted as the expected proportion correct p_e, can be very large. The p_e depends on the

number of categories and the number of cells in each category in S and A. Based on the observed proportion correct p_o and p_e, κ is defined as [60]:

$$\kappa = \frac{p_o - p_e}{1 - p_e} \tag{3}$$

Values for κ range from -1 (indicating no agreement for any of the cells) to 1 (indicating perfect agreement of S and A). If p_o is equal to p_e, i.e., if the land-use types are allocated randomly, κ is equal to 0. The κ coefficient tends to overestimate the performance of land-use change models, which use an initial land-use map as a starting point, if the number of actually changing cells is small compared to the number of cells with persistent land-use. In this case, a model that randomly allocates a small quantity of change, or simulates no change at all, can reach κ values close to 1. Hence, we also calculated the κ_{sim} coefficient, which considers the number of actual and simulated land-use transitions for the calculation of the expected proportion correct $p_{e(transition)}$. In order to calculate $p_{e(transition)}$, additionally the initial land-use map was considered. The value range for κ_{sim} is similar to that of κ and can be interpreted in the same way. Similarly to the standard κ, κ_{sim} is then defined as [60]:

$$\kappa_{sim} = \frac{p_o - p_{e(transition)}}{1 - p_{e(transition)}} \tag{4}$$

In order to calculate κ and κ_{sim}, the land-use categories in the simulated land-use map and the MODIS dataset were harmonized. For this purpose, the land-use categories that LandSHIFT.JR simulates explicitly, i.e., "urban land", "cropland", and "rangeland", were coded similarly in both maps. The remaining land-use types, e.g. "barren land", were lumped together in the categories "natural land-cover" or "water". Rangeland is not classified as a separate land-use type in the MODIS dataset. Therefore, we used the SRD map to derive the extent of rangeland. We defined a cell as rangeland if the density of small ruminants was 87 animals per km^2 or higher and at the same time the land-use/land-cover type assigned in the MODIS map was different from urban, cropland, and water. The threshold value of small ruminant density was adjusted in order to maximize κ. Since SRD is provided on a different spatial resolution (0.05 dd) and the conversion of SRD to "real" grazing land is very straightforward we consider the classification of rangeland to be rather inaccurate. Therefore, we tested the model performance based on two different sets of land-use maps. In set "UCR" urban, cropland, and rangeland were considered; in set "UC" only urban and cropland were considered as separate land-use categories.

For the "UCR" set, the validation results for the map comparison were 0.6 and 0.12 for κ and κ_{sim}, respectively. A value of κ=0.6 indicates that the agreement of the simulated and observed land-use map was significantly better than it can be expected for a random model. Compared to other studies, which report κ values from 0.6 to above 0.9 for land-use change modeling [36, 65], the agreement of LandSHIFT.JR results and the reference map was relatively low. However, it is important to bear in mind that we did not calibrate LandSHIFT.JR in order to maximize the agreement to observed datasets. The results are entirely based on parsimonious assumptions and objective methods to derive model parameters, e.g. the suitability factor weights. Hence, lower κ-values are to be expected.

The κ coefficient can be interpreted as the gain in agreement of the model as compared to a baseline assumption. For standard κ the baseline is a process that randomly allocates the proportion of categories given be the model. For κ_{sim}, the baseline is an improved random process using the additional information that possible changes in land use are limited to a certain, potentially very small, proportion of the cells, which is derived from the simulation results and the reference map. Therefore, the expected proportion correct increases for κ_{sim} and the values are generally lower. Hence, a κ_{sim} of 0.12 still indicates that LandSHIFT.JR explains the land-use changes in the study region significantly better than the improved baseline process.

When we used only the information originally given by the MODIS dataset (i.e. omitting the land-use type rangeland and using the set "UC") κ increased to 0.72 and κ_{sim} increased to 0.22. This can partly be attributed to the inaccuracies induced by the simple approach to derive the reference distribution of rangeland. Furthermore, it is important to consider that the reference map is derived from a remote sensing product (MODIS) and the small ruminant density dataset, which both are subject to classification and measurement errors. Additional sources of error may by introduced by data preparation, e.g. spatial aggregation (MODIS) and disaggregation (SRD).

6.3. Comparison with statistics

We compared the simulated area for rainfed and irrigated cropland for the year 2005 to estimates of the national statistical agencies of Israel, Jordan, and PA (Table 5). Although the model results for area under crops were in very good agreement for PA, the model simulated considerably higher area demands in Israel and Jordan (Table 5). For Israel, the simulated area demand for irrigated and rainfed cropland in 2005 was 48% and 66% higher than reported by the statistics, respectively. According to the Central Bureau of Statistics in Israel, the method to estimate the area under crops has changed starting in 2003. For that reason, a comparison to earlier years is not possible. However, LandSHIFT.JR uses the estimates of area under crops for the base year 2000 as an initial condition. Hence, the simulated area and the area reported by the statistics cannot be compared directly. For Jordan, the simulated area demand was overestimated by 41% and 57% for irrigated and rain-fed crops, respectively. This discrepancy can partly be explained by the fact that, according to the state statistics, the area under crops increased by only 4% while the production of agricultural products, which is the main driver of LandSHIFT.JR, increased by 46% [18]. Assuming that high-quality land resources are already in use for crop production, this is only possible if crop productivity increases considerably due to massive changes in agricultural management, e.g., fertilizer application or irrigation techniques. Currently, LandSHIFT.JR cannot simulate such effects because of missing input data. According to the MODIS land cover dataset for 2005 the area of cropland increased by about 63 %, which is more consistent with the relative increase in crop production simulated with LandSHIFT.JR.

7. Application example

In order to give an application example of LandSHIFT.JR, we set up a modeling exercise. As drivers for the model, we use the assumptions on the dynamics of population number,

	Rainfed cropland		Irrigated cropland		Total cropland	
	Statistics [km^2]	LandSHIFT.JR [km^2]	Statistics [km^2]	LandSHIFT.JR [km^2]	Statistics [km^2]	LandSHIFT.JR [km^2]
Israel	1283	2129 (+66%)	1298	1926 (+48%)	2581	4055 (+57%)
Jordan	1663	2613 (+57%)	610	858 (+41%)	2273	3471 (+53%)
PA	1545	1561 (+1%)	184	184 (0%)	1729	1745 (+1%)

Table 5. Area under rainfed and irrigated crops in 2005 for Israel, Jordan, and the Palestinian National Authority (PA) as simulated with LandSHIFT.JR and estimated by the national statistical agencies.

agricultural production, livestock production, and yield change due to technological progress as given by the GLOWA Jordan River *Modest Hopes* scenario [6]. Figure 4 shows the LandSHIFT.JR results for land-use/land-cover distribution, population density, and livestock density for the base year (2000) and the corresponding projections for the year 2050.

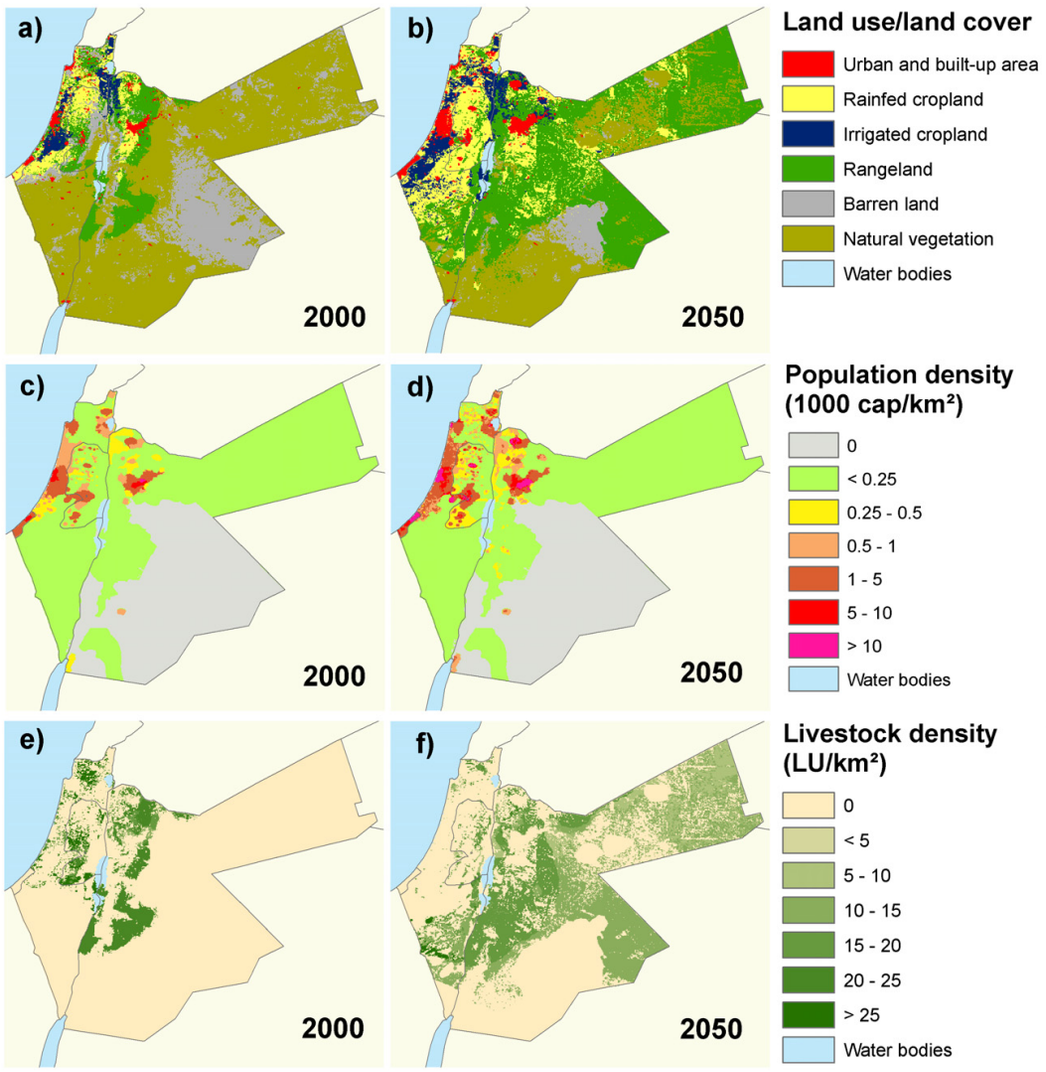

Figure 4. Maps of land-use and land-cover distribution, population density, and livestock density for the years 2000 and 2050 simulated with LandSHIFT.JR for the *Modest Hopes* scenario [6].

A comparison of Fig. 4 (a) and (b) shows considerable increases in the area demands for the main land-use activities. By 2050, the extent of urban land increases by about 56 %, while irrigated cropland expands to more than twice, rainfed cropland to more than three times, and grazing land to more than four times the area as compared to 2000. The figures for agricultural area reflect the ranking of the four activities: the lower the priority of a land-use activity is the lower is the productivity on the areas it is allocated to and, consequently, the larger is the area expansion needed to fulfill the demands. The increasing population density between 2000 and 2050 is shown in Fig. 4 (c) and (d). The maps show the typical differences between the modeling approaches for rural and urban population growth. On the one hand, the urban encroachment approach leads to relative fast growth of urban land (population density above 5000 people/km^2) at the edges of existing cities or urban centers. On the other hand, rural population density increases uniformly and proportional to the initial population density, which is distributed homogeneously over administrative units. Hence, the outlines of these districts can partly be recognized in the maps. The land-use activity with the lowest priority is grazing. Therefore, rangeland is more and more displaced from areas with relatively high productivity, where it is predominantly allocated in 2000 (Fig. 4 (e)), and shifted to less productive areas (Fig. 4 (f)). This leads to a vast extent of rangeland with low stocking densities in 2050. The expansion of irrigated cropland (Fig. 4 (a) and (b)) causes irrigation water requirements to rise. Table 6 presents the simulated total irrigation water demand and area specific irrigation water demand on state level. According to these figures, the projected irrigation water demand almost doubles in PA and Jordan and is about threefold in Israel in 2050 as compared to the year 2000.

State	IR water demand [10^6 m^3]		Avg. IR water demand [mm]	
	(2000)	(2050)	(2000)	(2050)
Israel	638	1477 (+132%)	31	72
Jordan	322	772 (+140%)	4	9
PA	86	162 (+88%)	14	26

Table 6. Total simulated (change between 2000 and 2050 in parenthesis) and average area specific irrigation water demand in 2000 and 2050 for Israel, Jordan, and the Palestinian National Authority (PA).

8. Discussion and conclusions

In this chapter, we introduce the integrated modeling system LandSHIFT.JR for the Jordan River region. We give a detailed description of the modeling system, its parameterization, and validation. We furthermore present a sample application of LandSHIFT.JR for the *Modest Hopes* scenario, developed in the context of the GLOWA Jordan River scenario exercise [6].

Since vegetation degradation due to overgrazing is a major problem in the Jordan River region [1] and since the intensity levels of grazing management strongly affect the environment via different pathways (e.g. woody encroachment [7], biodiversity loss [1] or erosion [27]) we developed a separate module for livestock grazing, that not only implements indicators for grazing intensity, but also includes different rangeland management strategies [28, 29]. This allows to consider the effect of rangeland management strategies in environmental impact assessments.

In contrast to earlier versions of LandSHIFT.JR, the current version includes the effect of changing climate conditions on crop yields and productivity of natural vegetation, which was shown to have a strong effect on land demand in the Jordan River region [32]. The indirect effect of productivity on area demand for the different agricultural activities is included indirectly by spatially explicit simulation models (WADISCAPE and GEPIC), driven by high-resolution climate change simulations for the Jordan River region [53]. This allows the inclusion of a high level of spatial detail into the simulations of land-use and land-cover change, which is carried out on a grid with a spatial resolution of 30 arc seconds. This is of high importance in a region with such high variability in biogeographic conditions as the Jordan River region. Furthermore, it applies a consistent assessment method to the entire Jordan River region and allows the combined assessment of socio-economic and climate impact on the food production systems in the Jordan River region which is considered to be mandatory [55, 56].

Another striking feature of the presented modeling system is the separate module for irrigated crop production. This module allows to simulate spatial and temporal dynamics of irrigated crop production and the resulting land-use patterns and intensities [32]. The model also enables an assessment of climate dependent net irrigation water requirements simulated with the GEPIC model. Hence, the modeling system can now be used the evaluate the effect of changes in cropland extent (induced by changing climate conditions and/or demands for agricultural commodities) on the net irrigation water requirements. However, it has to be mentioned that the current LandSHIFT.JR version only evaluates the demand and no connection to water supply is implemented so far. LandSHIFT.JR considers only crop categories and does not differentiate between crop types. The net irrigation water requirements for the different crop categories were inferred from GEPIC simulations for wheat yields using a crop-specific adjustment parameter. This approach introduces some inaccuracy into the simulation and, as a result, makes the simulation results more suitable for the evaluation of changes in water requirements as compared to the absolute amounts. Furthermore, no information on conveyance efficiencies or irrigation efficiencies (e.g. drip irrigation versus sprinkler irrigation) is included, which would be required to derive the gross irrigation water requirements.

In order to validate LandSHIFT.JR, three different validation methods were applied: (1) ROC analysis [43], (2) map comparison using κ and κ_{sim} as performance measures [42, 60], and (3) a comparison of the quantity of simulated land-use changes with observed land-use changes. The results for the ROC analysis (AUC = 0.81 for METRO, AUC = 0.84 for AGRO, and AUC = 0.83 for GRAZE) indicate that the suitability assessment in LandSHIFT.JR explains the location of change to a high degree. The validation results for the map comparison are at the lower range of values reported for land-use models, with 0.6 and 0.12 for κ and κ_{sim} (0.72 and 0.22 without rangeland), respectively. Bearing in mind that the modeling approach of LandSHIFT.JR does not include a calibration step (e.g. [50, 65]), but is entirely based on parsimonious assumptions and objective methods, we consider these values as acceptable. The comparison of observed and simulated land-use changes shows an almost perfect agreement for PA. Discrepancies resulting for Israel and Jordan might partly be induced by inconsistencies in the reported values. Based on the validation results, we consider LandSHIFT.JR suitable for the simulation of the location and quantity of land-use changes in the Jordan River region.

As shown for the application example, LandSHIFT.JR implements modules for the four land-use activities infrastructure and housing, irrigated crop production, rainfed crop production, and livestock grazing. For each land-use activity, besides the dominant land-use types also an indicator of land-use intensity is allocated (population density, irrigated or rainfed crop production amount, stocking density). Hence, the model concept implemented in LandSHIFT.JR considers not only land-use patterns, but also the corresponding land-use intensities. This makes LandSHIFT.JR land-use simulation results suitable for applications focusing on natural resource management and environmental impact assessment [24, 39].

We see a potential for improvement regarding the validation process. The spatially explicit validation of rangeland, net irrigation water requirements, and the separate validation of irrigated and rainfed cropland was limited by insufficient data availability. This will be caught up for, once suitable datasets are available. We encounter this validation issues by choosing a straightforward modeling approach, based on logical assumptions and renunciation of model calibration and consider this approach as second best to data.

In addition to extensive sensitivity and uncertainty analyses to improve the scientific knowledge and understanding of land-use systems in the Jordan River region, we see a strong potential for future studies on the relationship between irrigation water supply (including treated wastewater), net irrigation water requirements, and soil sensitivity towards the irrigation with treated wastewater [47]. For this purpose, additional GEPIC simulations for other crop types besides wheat would be required in order to be able to assess the irrigation water requirements more accurately. This would allow for interesting analyses regarding the potential of using treated wastewater for irrigation purposes, under consideration of possible environmental problems associated with the use of treated wastewater for irrigation [5].

Acknowledgments

This study is part of the GLOWA Jordan River project financed by the German Federal Ministry of Education and Research (FKZ 01LW0502). We thank Katja Geissler (Potsdam University, Research Group Plant Ecology and Nature Conservation) and Martin Köchy (Johann Heinrich von Thünen Insitut, Braunschweig) for the provision of WADISCAPE model output. Furthermore, we thank Gerhard Smiatek (IMK-IFU, Institute for Meteorology and Climate Research-Atmospheric Environmental Research) for the provision of regional climate simulation results.

Author details

Jennifer Koch, Florian Wimmer, Rüdiger Schaldach, Janina Onigkeit
Center for Environmental Systems Research, University of Kassel, Germany

9. References

[1] Abahussain, A.A., Abdu, A.S., Al-Zubari, W.K., El-Deen, N.A. & Abdul-Raheem, M. (2002). Desertification in the Arab region: analysis of current status and trends, *Journal of Arid Environments* 51(4):521–545.

[2] Alcamo, J. (2002). Three issues for improving integrated models: uncertainty, social science, and legitimacy, *in* Gethmann, C.F. & Lingner, S. (eds.), *Integrative Modellierung zum Globalen Wandel*, Springer Verlag, Berlin, Heidelberg, Germany, pp. 3–14.

[3] Alcamo, J. (2009). *Environmental futures: the practice of environmental scenario analysis*, Elsevier, Amsterdam, The Netherlands.

[4] Al-Jaloudy, M.A. (2001). *FAO country profiles: Jordan. Country pasture/forage resource profiles*, Food and Agriculture Organization of the United Nations, Rome, Italy. URL: `http://www.fao.org/ag/AGP/AGPC/doc/Counprof/Jordan/Jordan.htm`

[5] Al-Nakshabandi, G.A., Saqqar, M.M., Shatanawi, M.R., Fayyad, M. & Al-Horani, H. (1997). Some environmental problems associated with the use of treated wastewater for irrigation in Jordan, *Agricultural Water Management* 34(1):81–94.

[6] Anonymous (2011). *Future management of the Jordan River basin's water and land resources under climate change - a scenario analysis*, Summary report, Center for Environmental Systems Research, Kassel, Germany and Israel/Palestine Center for Research and Information, Jerusalem, Israel.

[7] Asner, G.P., Elmore, A.J., Olander, L.P., Martin, R.E. & Harris, A.T. (2004). Grazing systems, ecosystem responses, and global change, *Annual Review of Environment and Resources* 29:261–299.

[8] CIESIN (2004). *Global rural-urban mapping project (GRUMP): urban/rural population grids*, Center for International Earth Science Information Network, Columbia University, International Food Policy Research Institute, the World Bank & Centro Internacional de Agricultura Tropical. URL: `http://sedac.ciesin.columbia.edu/gpw/`

[9] Cohen, J. (1960). A coefficient of agreement for nominal scales, *Educational and Psychological Measurement* 20(1):37–46.

[10] Diakoulaki, D., Mavrotas, G. & Papayannakis, L. (1995). Determining objective weights in multiple criteria problems: the CRITIC method, *Computers & Operations Research* 22(7):763–770.

[11] Eastman, J.R., Jin, W., Kyem, P.A.K. & Toledano, J. (1995). Raster procedures for multi-criteria/multi-objective decisions, *Photogrammetric Engineering & Remote Sensing* 61(5):539–547.

[12] Erb, K.-H., Gaube, V., Krausmann, F., Plutzar, C., Bondeau, A. & Haberl, H. (2007). A comprehensive global 5 min resolution land-use data set for the year 2000 consistent with national census data, *Journal of Land Use Science* 2(3):191–224.

[13] EXACT (1998). *Overview of Middle East water resources*, Executive Action Team, Middle East Water Data Banks Project. URL: `http://exact-me.org/overview/index.htm`

[14] Falkenmark, M. & Rockström, J. (2004). *Balancing water for humans and nature: the new approach in ecohydrology*, Earthscan, London, United Kingdom.

[15] FAO (2003). *Review of world water resources by country*, Water Reports 23, Food and Agriculture Organization of the United Nations, Rome, Italy.

[16] FAO (2007). *Gridded livestock of the world 2007*, Food and Agriculture Organization of the United Nations, Rome, Italy.

[17] FAO (2012). *AQUASTAT: FAO's information system on water and agriculture*, Food and Agriculture Organization of the United Nations, Rome, Italy. URL: `http://www.fao.org/nr/water/aquastat/main/index.stm`

[18] FAO (2012). *FAO statistical database*, Food and Agriculture Organization of the United Nations, Rome, Italy. URL: `http://faostat.fao.org/`

[19] FIMA (2011). *RWDB2 River-surface water body network*, Food and Agriculture Organization of the United Nations, Aquaculture Management and Conservation Service (FIMA), Rome, Italy. URL: `http://www.fao.org/geonetwork/srv/en/main.home`

[20] Foley, J.A., DeFries, R., Asner, G.P., Barford, C., Bonan, G., Carpenter, S.R., Chapin, F.S., Coe, M.T., Daily, G.C., Gibbs, H.K., Helkowski, J.H., Holloway, T., Howard, E.A., Kucharik, C.J., Monfreda, C., Patz, J.A., Prentice, I.C., Ramankutty, N. & Snyder, P.K. (2005). Global consequences of land use, *Science* 309(5734):570–574.

[21] Friedl, M.A., McIver, D.K., Hodges, J.C.F., Zhang, X.Y., Muchoney, D., Strahler, A.H., Woodcock, C.E., Gopal, S., Schneider, A., Cooper, A., Baccini, A., Gao, F. & Schaaf, C. (2002). Global land cover mapping from MODIS: algorithms and early results, *Remote Sensing of Environment* 83(1-2):287–302.

[22] Ghasemi, F., Jakeman, A.J. & Nix, H.A. (1995). *Salinisation of land and water resources: human causes, extent, management and case studies*, Centre for Resources and Environmental Studies, Australian National University, CAB International, Wallingford, United Kingdom.

[23] Grimm, V., Berger, U., Bastiansen, F., Eliassen, S., Ginot, V., Giske, J., Goss-Custard, J., Grand, T., Heinz, S.K., Huse, G., Huth, A., Jepsen, J.U., Jørgensen, C., Mooij, W.M., Müller, B., Pe'er, G., Piou, C., Railsback, S.F., Robbins, A.M., Robbins, M.M., Rossmanith, E., Rüger, N., Strand, E., Souissi, S., Stillman, R.A., Vabø, R., Visser, U. & DeAngelis, D.L. (2006). A standard protocol for describing individual-based and agent-based models, *Ecological Modelling* 198(1-2):115–126.

[24] Gunkel, A. & Lange, J. (2012). New insights into the natural variability of water resources in the lower Jordan River basin, *Water Resources Management* 26(4):963–980.

[25] Haberl, H., Erb, K.-H., Krausmann, F., Gaube, V., Bondeau, A., Plutzar, C., Gingrich, S., Lucht, W. & Fischer-Kowalski, M. (2007). Quantifying and mapping the human appropriation of net primary production in earth's terrestrial ecosystems, *Proceedings of the National Academy of Sciences of the United States of America* 104(31):12942–12947.

[26] Kan, I., Rapaport-Rom, M. & Shechter, M. (2007). Economic analysis of climate-change impacts on agricultural profitability and land use: the case of Israel, *Proceedings of 15th Annual Conference of the European Association of Environmental and Resource Economists (EAERE)*, Thessaloniki, Greece, pp. 14-17.

[27] Khresat, S.A., Rawajfih, Z. & Mohammad, M. (1998). Land degradation in north-western Jordan: causes and processes, *Journal of Arid Environments* 39(4):623–629.

[28] Koch, J., Schaldach, R. & Köchy, M. (2008). Modeling the impacts of grazing land management on land-use change for the Jordan River region, *Global and Planetary Change* 64(3-4):177–187.

[29] Koch, J., Schaldach, R. & Kölking, C. (2009). Modelling the impact of rangeland management strategies on (semi-)natural vegetation in Jordan, *Proceedings of the 18th World IMACS Congress and MODSIM09 International Congress on Modelling and Simulation*, Cairns, Australia, pp. 1929–1935.

[30] Koch, J. (2010). *Modeling the impacts of land-use change on ecosystems at the regional and continental scale*, Thesis, kassel university press GmbH, Kassel, Germany.

[31] Koch, J., Onigkeit, J., Schaldach, R., Alcamo, J., Köchy, M., Wolff, H.-P. & Kan, I. (2011). Land-use change scenarios for the Jordan River region, *International Journal of Sustainable Water and Environmental Systems* 3(1):25–31.

[32] Koch, J., Wimmer, F., Schaldach, R., Onigkeit, J. & Folberth, C. (2012). Modelling the impact of climate change on irrigation area demand in the Jordan River region, *in* Seppelt, R., Voinov, A.A., Lange, S. & Bankamp. D. (eds.), *Proceedings of the 2012 International Congress on Environmental Modelling and Software: Managing Resources of a Limited Planet (iEMSs 2012)*, Leipzig, Germany.

[33] Köchy, M. (2008). Effects of simulated daily precipitation patterns on annual plant populations depend on life stage and climatic region, *BMC Ecology* 8(4).

[34] Köchy, M., Mathaj, M., Jeltsch, F. & Malkinson, D. (2008). Resilience of stocking capacity to changing climate in arid to Mediterranean landscapes, *Regional Environmental Change* 8(2):73–87.

[35] Lambin, E.F., Rounsevell, M.D.A. & Geist, H.J. (2000). Are agricultural land-use models able to predict changes in land-use intensity? *Agriculture, Ecosystems & Environment* 82(1-3):321–331.

[36] Lauf, S., Haase, D., Hostert, P., Lakes, T. & Kleinschmit, B. (2012). Uncovering land-use dynamics driven by human decision-making - a combined model approach using cellular automata and system dynamics, *Environmental Modelling & Software* 27-28:71–82.

[37] Liu, J., Williams, J.R., Zehnder, A.J.B. & Yang, H. (2007). GEPIC - modelling wheat yield and crop water productivity with high resolution on a global scale, *Agricultural Systems* 94(2):478–493.

[38] Malkinson, D. & Jeltsch, F. (2007). Intraspecific facilitation: a missing process along increasing stress gradients - insights from simulated shrub populations, *Ecography* 30(3):339–348.

[39] Menzel, L., Koch, J., Onigkeit, J. & Schaldach, R. (2009). Modelling the effects of land-use and land-cover change on water availability in the Jordan River region, *Advances in Geosciences* 21:73–80.

[40] Perevolotsky, A., Landau, S., Kababia, D. & Ungar, E.D. (1998). Diet selection in dairy goats grazing woody Mediterranean rangeland, *Applied Animal Behaviour Science* 57(1-2):117–131.

[41] Pimm, S.L. & Raven, P. (2000). Biodiversity: extinction by numbers, *Nature* 403:843–845.

[42] Pontius Jr., R.G. (2000). Quantification error versus location error in comparison of categorical maps, *Photogrammetric Engineering & Remote Sensing* 66(8):1011–1016.

[43] Pontius Jr., R.G. & Schneider, L.C. (2001). Land-cover change model validation by an ROC method for the Ipswich watershed, Massachusetts, USA, *Agriculture, Ecosystems & Environment* 85(1-3):239–248.

[44] Portmann, F.T., Siebert, S. & Döll, P. (2010). MIRCA2000 - Global monthly irrigated and rainfed crop areas around the year 2000: a new high-resolution data set for agricultural and hydrological modeling, *Global Biogeochemical Cycles* 24:GB1011.

[45] Rosegrant, M.W., Meijer, S. & Cline, S.A. (2002). *International model for policy analysis of agricultural commodities and trade (IMPACT): model description*, International Food and Policy Research Institute, Washington, DC, United States. URL: `http://www.ifpri.org/themes/impact/impactmodel.pdf`

[46] Saaty, R.W. (1987). The analytic hierarchy process - what it is and how it is used, *Mathematical Modelling* 9(3-5):161–176.

[47] Schacht, K., Gönster, S., Jüschke, E., Chen, Y., Tarchitzky, J., Al-Bakri, J., Al-Karablieh, E. & Marschner, B. (2011). Evaluation of soil sensitivity towards the irrigation with treated wastewater in the Jordan River region, *Water* 3(4):1092–1111.

[48] Schaldach, R. & Koch, J. (2009). Conceptual design and implementation of a model for the integrated simulation of large-scale land-use systems, *in* Athanasiadis, I.N., Mitkas, P.A., Rizzoli, A.E. & Gómez, J.M. (eds.), *Information Technologies in Environmental Engineering*, Springer Verlag, Berlin, Heidelberg, Germany, pp. 425–438.

[49] Schaldach, R., Alcamo, J., Koch, J., Kölking, C., Lapola, D.M., Schüngel, J. & Priess, J.A. (2011). An integrated approach to modelling land-use change on continental and global scales, *Environmental Modelling & Software* 26(8):1041–1051.

[50] Schweitzer, C., Priess, J.A. & Das, S. (2011). A generic framework for land-use modelling, *Environmental Modelling & Software* 26(8):1052–1055.

[51] Seré, C. & Steinfeld, H. (1996). *World livestock production systems - current status, issues and trends*, FAO Animal Production and Health Paper 127, Food and Agriculture Organization of the United Nations, Rome, Italy.

[52] Siebert, S., Döll, P., Feick, S., Hoogeveen, J. & Frenken, K. (2007). *Global Map of Irrigation Areas version 4.0.1*, Johann Wolfgang Goethe University, Frankfurt am Main, Germany/Food and Agriculture Organization of the United Nations, Rome, Italy.

[53] Smiatek, G., Kunstmann, H. & Heckl, A. (2011). High-resolution climate change simulations for the Jordan River area, *Journal of Geophysical Research* 116:D16111.

[54] Solecki, W.D. & Oliveri, C. (2004). Downscaling climate change scenarios in an urban land use change model, *Journal of Environmental Management* 72(1-2):105–115.

[55] Tubiello, F.N., Soussana, J.-F. & Howden, S.M. (2007). Crop and pasture response to climate change, *Proceedings of the National Academy of Sciences of the United States of America* 104(50):19686–19690.

[56] Tubiello, F.N., Amthor, J.S., Boote, K.J., Donatelli, M., Easterling, W., Fischer, G., Gifford, R.M., Howden, M., Reilly, J. & Rosenzweig, C. (2007). Crop response to elevated CO_2 and world food supply: a comment on "Food for Thought ..." by Long et al., Science 312:1918–1921, 2006, *European Journal of Agronomy* 26(3):215–223.

[57] Uchida, H. & Nelson, A. (2008). *Agglomeration index: towards a new measure of urban concentration*, Background Paper, World Development Report 2009.

[58] UNEP (2007). *Global Environment Outlook - environment for development (GEO-4)*, United Nations Environment Programme, Nairobi, Kenya.

[59] U.S. Geological Survey (1998) *HYDRO1k: elevation derivative database*, Earth Resources Observation and Science (EROS) Center, Sioux Falls, SD, United States. URL: `http://eros.usgs.gov/#/Find_Data/Products_and_Data_Available/gtopo30/hydro`

[60] van Vliet, J., Bregt, A.K. & Hagen-Zanker, A. (2011). Revisiting Kappa to account for change in the accuracy assessment of land-use change models, *Ecological Modelling* 222(8):1367–1375.

[61] Verburg, P.H., de Koning, G.H.J., Kok, K., Veldkamp, A. & Bouma, J. (1999). A spatial explicit allocation procedure for modelling the pattern of land use change based upon actual land use, *Ecological Modelling* 116(1):45–61.

[62] Verburg, P.H., Soepboer, W., Veldkamp, A., Limpiada, R., Espaldon, V. & Mastura, S.S.A. (2002). Modeling the spatial dynamics of regional land use: the CLUE-S model, *Environmental Management* 30(3):391–405.

[63] Verburg, P.H., Kok, K., Pontius, R.G. & Veldkamp, A. (2006). Modeling land-use and land-cover change, *in* Lambin, E.F. & Geist, H.J. (eds.), *Land-use and land-cover change - local processes and global impacts*, Springer Verlag, Berlin, Heidelberg, Germany, pp. 117–135.

[64] Vitousek, P.M. (1994). Beyond global warming: ecology and global change, *Ecology* 75(7):1861–1876.

[65] Wang, F., Hasbani, J.-G., Wang, X. & Marceau, D.J. (2011). Identifying dominant factors for the calibration of a land-use cellular automata model using Rough Set Theory, *Computers, Environment and Urban Systems* 35(2):116–125.

[66] WDPA Consortium (2004) *Word Database on Protected Areas.* URL: `http://www.wdpa.org/`

[67] Williams, J.R., Jones, C.A., Kiniry, J.R. & Spanel, D.A. (1989). The EPIC crop growth model, *Transactions of the American Society of Agricultural Engineers* 32(2):497–511.

[68] Williams, J.R. (1995). The EPIC model, *in* Singh, V.P. (ed.), *Computer Models of Watershed Hydrology*, Water Resources Publications, Colorado, United States, pp. 909–1000.

[69] Wu, F. (1999). GIS-based simulation as an exploratory analysis for space-time processes, *Journal of Geographical Systems* 1(3):199–218.